Published in final edited form as:
Eur J Cell Biol. 2008 September ; 87(8-9): 555–567. doi:10.1016/j.ejcb.2008.02.008.

A role for the podosome/invadopodia scaffold protein Tks5 in tumor growth in vivo

Barbara Blouw[a], **Darren F. Seals**[b], **Ian Pass**[a], **Begoña Diaz**[a], and **Sara A. Courtneidge**[a,*]

a*Burnham Institute for Medical Research, Tumor Microenvironment Program, 10901 North Torrey Pines Road, La Jolla, California 92037, USA*

b*Wake Forest University School of Medicine, Department of Cancer Biology, Winston-Salem, North Carolina 27157, USA*

Abstract

Podosomes and invadopodia are electron-dense, actin-rich protrusions located on the ventral side of the cellular membrane. They are detected in various types of normal cells, but also in human cancer cells and in Src-transformed fibroblasts. Previously we have shown that the scaffold protein Tks5 (tyrosine kinase substrate 5) co-localizes to podosomes/invadopodia in different human cancer cells and in Src-transformed NIH-3T3 cells. Upon reduced expression of Tks5 podosome formation is decreased, which leads to diminished gelatin degradation in vitro in various human cancer cell lines. It is unclear, however, whether cancer cells need podosomes for tumor growth and metastasis in vivo. To test this idea, we evaluated the ability of Srctransformed NIH-3T3 cells, showing stable reduced expression of Tks5 and podosome formation (Tks5 KD), to form subcutaneous tumors in mice. We demonstrate that decreased expression of Tks5 correlated with reduced tumor growth at this site. In addition, we generated lung metastases from these cells following tail vein injection. The lungs of mice injected i.v. with the Tks5 KD showed smaller-sized metastases, but there was no difference in the number of lesions compared to the controls, indicating that podosomes may not be required for extravasation from the blood stream into the lung parenchyma. Independent of the microenvironment however, the reduced tumor growth correlated with decreased tumor vascularization. Our data potentially implicate a novel role of podosomes as mediators of tumor angiogenesis and support further exploration of how podosome formation and Tks5 expression contribute to tumor progression.

Keywords

Podosomes; Invadopodia; Tks5/Fish; Metastasis; Tumor growth; Angiogenesis

Introduction

Despite significant improvements in the treatment of cancer, the occurrence and growth of distant metastases is the major cause of morbidity and mortality. Metastasis is a multi-step process. At the primary site, tumor cells invade into the lymphatic system, or directly into the circulation. This is a result of extracellular matrix degradation followed by migration. Once in

*__Corresponding author:__ Phone: ++858 646 3128; E-mail address: courtneidge@burnham.org (S.A. Courtneidge).

the bloodstream, tumor cells must survive and avoid attacks by the immune cells to extravasate and colonize a distant organ. There, adequate blood supply will have to be established, allowing the metastatic tumor to grow (Steeg, 2006). Growing evidence has implicated specialized subcellular structures, called podosomes or invadopodia, in extracellular matrix degradation, and raised the interesting question of whether invadopodia are involved in metastasis in vivo.

Podosomes/invadopodia are highly dynamic, actin-rich adhesion structures localized on the ventral side of the cellular membrane. They are regulated by various proteins, including the Arp2/3 complex, N-WASp, WAVE1, Cdc42, ASAP1, cortactin, gelsolin, and cofilin (Bowden et al., 1999, 2006; Baldassarre et al., 2003; Yamaguchi et al., 2005; Artym et al., 2006; Chellaiah, 2006; Bharti et al., 2007; Clark et al., 2007). Podosomes/invadopodia are found in various mammalian cells such as macrophages, osteoclasts and vascular smooth muscle cells (Linder and Aepfelbacher, 2003). They are also detected in various human cancer cells, including breast, colon, and head and neck cancer cell lines (Artym et al., 2006; Bharti et al., 2007; Clark et al., 2007; Vishnubhotla et al., 2007) and in Src-transformed fibroblasts (Abram et al., 2003). The activation of Src is essential for the formation of these structures (Weaver, 2006).

Even though podosomes and invadopodia contain the same molecular components with virtually the same function, it is currently not clear whether podosomes and invadopodia truly represent distinct structures. We anticipate that this will be clarified by detailed examination in the near future. Until then, the convention is to use the term “podosome” for the structures found in normal cells (such as monocytic cells, endothelial cells and smooth muscle cells) and in Src-transformed fibroblasts, whereas the structures found in cancer cells are referred to as “invadopodia” (see (Gimona et al., 2008)). For the remainder of the manuscript we will adhere to this convention.

Several lines of evidence support the notion that podosomes/invadopodia play a critical role in tumor progression. First, in human cancer the expression of some of the proteins that regulate podosomes, such as Arp2/3, WASP, cortactin, gelsolin, and cofilin correlates with the occurrence of metastasis (Vignjevic and Montagnac, 2008). Second, in vitro studies have indicated that these proteins are involved in cancer cell invasion. In head and neck cancer cells, a reduced ability to form invadopodia was correlated with a decrease in matrigel invasion. This was correlated with a diminished secretion of metalloproteinases such as MMP9 and MMP2 (Clark et al., 2007). In contrast, similar experiments in Src-transformed fibroblasts, did not reveal alterations in the secretion of these metalloproteinases; however the activity of these gelatinases was compromised. It is also possible that podosomes/invadopodia in different cells secrete different proteases. This is supported by the observation that exposure to a cocktail of different protease inhibitors led to a similar decrease in invasion as reducing invadopodia formation alone (Seals et al., 2005). Possibly the molecules that regulate these structures have distinct roles in the secretion and activation of different proteases. In this regard it is important to note that even though in all cell types podosome/invadopodia formation was reduced, this was achieved by decreasing the expression of different genes, either cortactin (Clark et al., 2007), or Tks5 (Seals et al., 2005). It is incompletely understood how these proteins mediate the secretion and activation of pro-invasive molecules.

The role of podosomes during cancer cell invasion is generally tested using cells in which the expression of the proteins that regulate podosomes is reduced. Some of these molecules, however, such as cortactin, cofilin and Arp2/3 also regulate actin polymerization through direct interactions (Gimona and Buccione, 2006). Thus, alterations in the expression of some of these proteins might also affect the actin cytoskeletal morphology. This makes it difficult to establish whether specific alterations in podosome formation, or in the actin cytoskeleton, determine the phenotype that is being observed.

Previously, our lab has identified a new Src substrate and scaffold protein named Tks5/Fish (tyrosine kinase substrate 5) (Lock et al., 1998). For the remainder of the manuscript we will refer to this protein as Tks5. We showed that Tks5 co-localizes to podosomes in Src-transformed fibroblasts and that specific members of the ADAMs family of proteases, namely ADAM12, -15 and -19 bind to the fifth Src homology 3 (SH3) domain of Tks5 (Abram et al., 2003). More recently, we demonstrated that Tks5 is required for podosome formation and invasion in vitro, not only in Src-transformed fibroblasts but also in various human cancer cell lines. Tks5 does not contain known actin-binding sites, nor has it been shown to directly interact with the actin cytoskeleton. Furthermore, a variety of highly invasive tumor types such as breast cancer and melanoma showed a marked increase in the expression of Tks5 compared to normal breast tissue and skin (Seals et al., 2005).

To determine whether podosomes are also important during tumor growth and metastasis in vivo, we grew the Src-transformed fibroblasts in which the expression of Tks5 is stably reduced by 70–80%, and non-targeted controls, as subcutaneous tumors and lung metastases in mice. Here we report the results of these experiments.

Materials and methods

Cell lines and growth curve

The Src-transformed NIH-3T3 cells in which the expression of Tks5 was stably reduced have been described before in (Seals et al., 2005). For the growth curve, cells were plated at a concentration of 3×10^4 cells per well in triplicates, in a 12-well plate in either 10% or 1% fetal bovine serum (FBS). Cells were harvested every 24 h by trypsinization. At least 100 cells from each well were counted with a hemocytometer and the average cell number was determined. The growth curve was repeated three times and the values described in the figures are representative of one triplicate culture experiment ± the standard error of the mean (SEM).

Extracellular matrix degradation assay and fluorescence microscopy

Fluorescently-labeled gelatin-coated coverslips were prepared as described by Berdeaux et al. (2004), as originally described by Bowden et al. (1999). In brief, coverslips were coated with Oregon green 488-conjugated gelatin (Chemicon, Temecula, CA), cross-linked 15 min in 0.5% glutaraldehyde in phosphate-buffered saline (PBS), and incubated for 3 min with 5 mg/ml $NaBH_4$ in PBS. After quenching with Dulbecco's modified Eagle medium (DMEM) at 37°C, cells were plated on coated coverslips in DMEM (Invitrogen, Carlsbad, CA) containing 10% FBS and incubated for 3 to 4 h before processing for immunofluorescence. The detection of Tks5 expression and podosomes was carried out according to (Seals et al., 2005).

Subcutaneous tumor growth and lung metastasis assay

All animal experiments were conducted in accordance with the NIH Guide for the Care and Use of Laboratory Animals. Subcutaneous implantation was carried out as described in (Blouw et al., 2003). In short, cells were harvested by trypsinization and resuspended in PBS (Invitrogen) to a final concentration of 4×10^5 cells/ml. Athymic nude mice were injected in the flank with 100 µl for each cell line, and tumors were allowed to form for 14 days. Tumor growth was measured every 2–3 days using calipers, both the longest (L) and shortest (S) measurements were recorded. Using these values, tumor volumes were calculated as follows: $(L \times S^2) \times 0.5$ and expressed as mean volume ± SEM. Mice were sacrificed when the tumors reached a diameter of ~2 cm, according to the Animal Care and Use Policy of Burnham Institute of Medical Research. These experiments were repeated 3 times, using 4 to 8 mice per tumor group. For the lung metastasis assay, cells were collected as described above and resuspended at a final concentration of 5×10^6 cells/ml in PBS. Of this suspension, 100 µl was injected into the tail veins of athymic nude mice. Mice were observed for signs of tumor burden such as loss

of weight and a hunched back. After 17 days, the mice were sacrificed and the lungs were dissected out. This experiment was repeated 3 times using 5 to 8 mice per group. In all experiments, athymic mice were purchased from Harlan (Indianapolis, Indiana).

Tissue processing and immunohistochemistry

Prior to dissection of the subcutaneous tumors and lungs, mice were randomized for differential tissue processing. One third of the tumors/lungs of each group was used, respectively, for overnight fixation in 4% paraformaldehyde/PBS followed by paraffin embedding, one third was immediately flash frozen in liquid N_2 and one third was immediately embedded in OCT on dry ice (TissueTek, Torrance, CA).

To determine tumor cell proliferation, 5 μm thick paraffin sections were cut and subsequently stained with an antibody detecting proliferating cell nuclear antigen (PCNA) at 1:100 (BD Biosciences, San Jose, CA) in antibody diluent. The primary antibody was biotinylated using a biotinylation kit according to the manufacturer's instructions and developed in DAB (all reagents from Dako, San Jose, CA). This was followed by a counterstain using Methylgreen (Vectorlabs, Burlingame, CA).

Frozen sections were cut at 7 to 10 μm thickness and stained for immunofluorescence using a mouse monoclonal anti-Tks5 antibody at 1:10 (generated against the 4^{th} SH3 domain by the Courtneidge lab) followed by a secondary antibody, Alexafluor-594-conjugated anti-mouse (Chemicon) at 1:200. Finally, sections were counter stained with Hoechst 33258 to identify the nuclei (Sigma, St. Louis, MO) at 1:10,000 in PBS. All reagents were diluted in the components provided by the MOM kit (Vectorlabs). To determine vessel morphology and density, frozen sections were stained with mouse anti-CD31 (BD Biosciences) at 1:100. Next, a secondary antibody, Alexafluor-594-conjugated anti-mouse (Chemicon) was applied at 1:100. The antibodies were diluted in diluent from Dako. To detect metastatic lesions, paraffin-embedded lungs were serial-sectioned at 5 μm per section. Section number 25, which was approximately at the middle of the lung (each lung appeared to consist of ~50 sections), was subjected to standard hematoxylin and eosin (H&E) staining to determine the number and size of lesions as described below. Photographs were taken with a 4× objective. To determine cell death, apoptotic cells of both frozen and paraffin sections were detected using the ApopTaq Flourescein Direct In Situ Apoptosis Detection Kit purchased from Chemicon according to the manufacturer's instructions. Nuclei were identified as described above.

Photographs of Tks5 immunofluorescence and apoptosis were taken at a magnification of 200× on an Axioplan 2 fluorescence microscope and were analyzed with Axiovision 3.0 software (Zeiss). Images of the PCNA and CD31 staining were taken at magnifications of 100× and 200×, respectively. The photographs of the H&E images were taken at a magnification of 40×. All these images were taken with an inverted TE300 Nikon Fluorescence Microscope with a CCD Spot RT Camera using Spot RT Acquisition and Processing Software (Diagnostic Instruments Inc, Sterling Heights, MI).

Quantification of histological assays and statistical analysis

For the quantification of the proliferation rate, apoptotic rate, cellular density, vessel density and dilation, ImagePro software was used (MediaCybernetics, Bethesda, MD). For each analysis, tumors/lungs obtained from at least 2 to 3 different mice per group were used, and at least 6 to 7 photographs were taken per tumor/lung. Images were calibrated for the correct objective and the number of 'dark objects' (in the case of PCNA staining) or 'bright objects' (for the apoptotic rate and vessel density) were normalized to the total number of nuclei (indicated by Hoechst staining). Values were expressed as percentage per field. In the case of the lung metastasis assay, the values were normalized to the total number of nuclei in the metastatic

lesion, to ensure proper comparisons between lesions of different size. The average vessel diameter was measured by tracking at least 30 vessels per image, after which the software calculated the average width in μm. In the subcutaneous tumors, the values were expressed as average vessel width per field, whereas in the lung they were normalized to the area of metastatic lesion and expressed as width per mm^2 tumor tissue (both ± SEM).

To determine the size and number of metastatic lesions, images of at least 4 lungs per tumor groups were taken using Spot RT Acquisition and Processing Software. Images were calibrated for the 4× objective, and the metastatic lesions (indicated by blue color) were tracked after which the area in μm^2 was calculated. The entire lung was examined for lesions, and the metastatic size is expressed as total area of metastatic lesion per lung, whereas the density is expressed as total number of metastatic lesions per lung.

In all scatter plots, values are represented as the mean ± SEM unless otherwise noted. For statistical analysis, the Student's *t* test was used and p values that were equal or less than 0.05 were considered statistically significant.

Results

Reduced expression of Tks5 in Src-transformed NIH-3T3 cells leads to a decrease in subcutaneous tumor growth

For cancer cells to form a tumor, it is necessary to degrade the extracellular matrix. This not only fulfills a spatial requirement for tumor growth, but also allows the tumor to attract various cells from the microenvironment that provide favorable conditions for tumor growth, such as endothelial cells, fibroblasts and macrophages (Bingle et al., 2002; Orimo and Weinberg, 2006). Previously it has been shown that various types of human cancer cells form invadopodia. Furthermore, it was demonstrated that invadopodia possess proteolytic activity (reviewed in (Gimona and Buccione, 2006; Weaver, 2006)).

Previously our lab identified a new Src substrate named Tks5 (Lock et al., 1998). It contains an amino-terminal Phox-homology (PX) domain and five SH3 domains (Fig. 1A). Tks5 co-localizes to podosomes/invadopodia in various human cancer cells and in Src-transformed NIH-3T3 cells (indicated by white arrows in Fig. 1B top panel, and described by (Abram et al., 2003; Seals et al., 2005)). Furthermore, podosomes mediate the degradation of FITC-gelatin in vitro (arrows in Fig. 1B lower panels and as described by (Seals et al., 2005)). Earlier we generated Src-transformed fibroblasts in which Tks5 was stably reduced by 70–80% using short hairpin RNA (shRNA) technology (called Tks5 knockdown, or Tks5 KD cells). Compared to the control cells, which express a control, non-targeting, shRNA sequence, both podosome formation and gelatin degradation was decreased in the Tks5 KD cells (Seals et al., 2005), even though proliferation was unaffected (Fig. 1C, D). These observations led us to believe that podosomes might be required for tumor growth.

To test this hypothesis, the Tks5 KD cells and their controls were grown as subcutaneous tumors in immunocompromised mice as described in Materials and methods. In the mice implanted with the control cells (C1, C2), tumors were observed for the first time at 9 days post injection (Fig. 2A, B), whereas in the Tks5 KD group (4.20, 4.24), tumors were first observed 3 to 5 days later (Fig. 2 C, D). This delay in tumor growth was maintained until the end point of the assay, which was at day 14. As depicted in Figure 2E and F, at day 14, the tumors derived from clones 4.20 and 4.24 had a 2.5- to 7.4-fold reduction in volume compared to those derived from C1 and C2 ($p < 0.05$ comparing the volume of each knockdown tumor type with each of the controls by Student's *t* test). To test whether the reduced tumor volume correlated with a decreased expression of Tks5 in the KD tumors, cryo-sections were subjected to immunofluorescence using an antibody directed against Tks5. As shown in Figure 3A, most

KD tumor cells showed reduced Tks5 staining, with only a few expressing Tks5 at levels comparable to those in the tumors derived from controls (compare cells showing intense red staining in the KD and control tumors).

Under standard and growth factor-reduced tissue culture conditions, Tks5 knockdown did not influence the proliferation rate of the Tks5 KD cells compared to controls ((Seals et al., 2005) and see Fig. 1C, D). When grown in vivo however, a reduction in proteolytic activity could hamper the ability of the Tks5 KD tumors to propagate and expand, possibly explaining the reduced volume. To investigate whether this was the case, sections were examined for proliferation rate and for the number of cells observed in a specific field. To determine the proliferation rate, paraffin sections were stained with an antibody detecting PCNA, which is a marker for cells undergoing mitosis. Values were normalized to the number of cells per field. As shown in Figure 3B, a significant percentage of cells were mitotic in all tumors, with proliferation rates ranging from 58.7 to 72.3%. In keeping with the in vitro findings, no differences were observed between the proliferation rate of tumors derived from Tks5 KD and control clones (Fig. 3C). To establish whether there were differences in the cellular density of the tumors, cryo-sections were stained with Hoechst and photographs taken with a 100× objective were analyzed for the number of nuclei as described in Materials and methods. As shown in Figure 3D, no clear differences were observed between the tumors from Tks5 KD and control clones. Only when 4.24 tumors were compared with C2 tumors did we detect a reduction in the number of cells per field (~ 30%, which was significant by Student's *t* test $p < 0.05$). A reduced tumor volume can also be the result of an increase in cell death; therefore sections were analyzed for the percentage of apoptotic cells. Even though the apoptotic rate was low in all tumor types, as indicated by the small fraction of TUNEL-positive cells (means ranging from 0.5 to 1.4%, Figure 3E), there was a trend towards increased apoptosis in the Tks5 KD tumors compared to the controls (Fig. 3F).

Decreased angiogenesis in Tks5 KD tumors

During the dissection it appeared that compared to the controls, the Tks5 KD tumors were less hemorrhagic (Fig. 2F) and had a firmer texture, containing less edema (data not shown). These phenomena can be a result of reduced angiogenesis associated with an increased endothelial cell proliferation, vessel permeability and dilation. To determine whether Tks5 might be required for some aspect of angiogenesis, cryo-sections of knockdown and control tumors were stained with an antibody directed against CD31, a marker expressed by endothelial cells (Blouw et al., 2007). As shown in Figure 4A–C, the control tumors showed a more dense vessel network and an increased vessel dilation compared to the Tks5 KD tumors (compare the vessels indicated by white arrows of controls and Tks5 KD). The vessel density was determined from 6 to 8 fields per tumor type and two tumors per group. This analysis revealed that the Tks5 KD tumors had a reduction in vessel density compared to the controls, ranging from 1.4- to 2.4-fold (Fig. 4B). Next the average vessel diameter per tumor of at least 30 vessels per field, at 6 fields per tumor, and two tumors per group was examined. As shown in Figure 4C, the vessel diameter in the Tks5 KD tumors was reduced ~1.6- to ~2.8-fold compared to the control tumors. These data indicate that Tks5 might be involved in tumor angiogenesis.

Reduced expression of Tks5 decreases the size and vascularization of metastatic lesions

For cancer cells to disseminate from the tumor, and metastasize to and grow in a distant organ, extracellular matrix degradation is thought to be required. We next hypothesized that Tks5 may mediate metastasis. To test this idea, we used tail vein injection of tumor cells as a model of experimental metastasis. In this assay, tumor cells are tested for their ability to extravasate from the vasculature to colonize the lung. We introduced the Tks5 KD and control clones into the tail vein of immunocompromised mice and let lung metastases form for 17 days as described in Materials and methods. Over a 17-day time period, the mice injected with the control cells

showed an increased morbidity compared to the mice that received the Tks5 KD cells (data not shown), indicating a decreased ability to form lung metastasis in the latter. Indeed, as depicted in Figure 5A, upon dissection, the tumor lesions in the lung appeared more numerous and larger in the control tumors compared to the Tks5 KD tumors (compare the size of encircled tumor nodules). After processing the lungs for histological analysis, a more detailed examination of the number and size of the metastatic lesions was carried out. Lungs were cut in serial sections, followed by H&E staining which distinguishes the tumor nodules from the normal lung parenchyma. The same section number of each lung was examined for the number of lesions as well as the area of each lesion. As shown in Figure 5B, 4.24 seemed to be able to generate more metastatic lesions compared to 4.20 and the control cells, but no significant differences were observed between the different groups (Student's *t* test). In contrast, the size of the lesions was significantly reduced in all Tks5 KD tumors, ranging from 1.5- to 17-fold, compared to C1 but not C2 controls (Fig. 5C).

To test whether these data correlated with a reduced expression of Tks5 in the lung tumor nodules, sections were analyzed by immunofluorescence using an anti-Tks5 antibody. In keeping with our findings on the subcutaneous tumors, the fraction of cells expressing high levels of Tks5 appeared decreased in the Tks5 KD lung metastases compared to the controls (Fig. 5D). Next, we investigated whether disparities in proliferation or apoptosis could explain the difference in size of the metastatic lesions. Lung sections were analyzed for these factors similarly as described for the subcutaneous tumors. However, the metastases generated by the control cells were larger than those of the Tks5 KD cells (Fig. 5C). In order to adequately compare data obtained from tumor nodules that were different in size, we normalized the numbers obtained in analysis for the apoptotic and proliferation rate to the number of cells present in the lesion as opposed to the number of cells detected in the entire image. As shown in Figure 6A, cell death was strikingly low in all the metastatic lesions and the apoptotic rate was not different between the tumor groups. Similar to the subcutaneous data, the proliferation rate was high in all tumor groups and no clear differences were observed (Fig. 6B).

Next we asked whether the difference in metastatic size was associated with a decrease in vascularization, as was earlier described for the subcutaneous tumors. Lung sections were analyzed for both vessel density and dilation. For quantification of the vessel density, the total number of vessels was normalized to the area of lung metastatic nodule as described in Materials and methods. As shown in Figure 6C–E, the lung metastases generated by the Tks5 KD cells showed a trend towards reduced vascularization. The vessel density was decreased 2- to 6-fold in the Tks5 KD lesions compared to the controls (Fig. 6D). Furthermore, the vessel dilation was reduced 1.4- to 1.7-fold in the Tks5 KD metastases compared to the controls (Fig. 6E).

These data suggest that maintaining Tks5 expression in Src-transformed NIH-3T3 cells is not required for the cells to enter the lung from the bloodstream, as evidenced by the high number of micro-metastases in the 4.24 tumor group. Nevertheless, independent of the microenvironment, tumor growth was reduced in cells with a decreased expression of Tks5. Clear differences in cell death, proliferation and cellular density of the Tks5 KD and controls were not observed. However, the Tks5 knockdown tumors show a trend towards reduced tumor vascularization.

Discussion

Podosomes (called invadopodia in human cancer cells) are actin-rich protrusions that are located on the ventral side of the cellular membrane. They are found in a number of different invasive human cancer cell lines, and also in Src-transformed NIH-3T3 cells (Gimona et al., 2008). In the latter, the podosomes cluster to form rings or semi-circles that are called rosettes.

Using in vitro assays, several groups have shown that podosomes/invadopodia mediate degradation of the extracellular matrix (Seals et al., 2005; Artym et al., 2006; Clark et al., 2007). Although it is generally thought that extracellular matrix degradation is essential for tumor growth and metastasis, it is unclear whether podosomes/invadopodia mediate this process in vivo (Weaver, 2006). We have demonstrated previously that the scaffold protein Tks5 co-localizes to podosomes in Src-transformed fibroblasts. When the expression of Tks5 is reduced, podosome formation is decreased without affecting actin polymerization and the integrity of the cytoskeleton (Seals et al., 2005). We therefore reasoned that analyzing the growth of cells in which Tks5 is stably reduced as subcutaneous tumors and lung metastases could help determine the role of podosome formation during tumor growth.

Our data suggest that a diminished ability to form podosomes and degrade extracellular matrix in vitro, mediated by a decrease in Tks5 expression, correlates with impaired tumor growth of Src-transformed NIH-3T3 cells. This is also correlated with a reduction in tumor vascularization as revealed by a decreased vessel density and vessel dilation. Our observations could not be fully explained by differences in proliferation or apoptosis. In keeping with this, it was recently reported that invadopodia are not important for cell viability (Weaver, 2006; Vishnubhotla et al., 2007). However, we only analyzed tumors that were isolated at the end point of the assay, which may have masked differences in cell death and proliferation that occurred at an earlier stage. This could be clarified by the examination of tumor samples isolated at an earlier time point.

Tks5 knockdown does not seem to impair the ability of cells to metastasize to the lung, as indicated by the high number of micro-metastases generated by the 4.24 Tks5 KD cells. In our assay however, the cells were introduced through the tail vein. Once in the lung capillaries, cells arrest, extravasate into the surrounding tissue and establish tumor growth. It is incompletely understood how cells accomplish this process after being injected into the tail vein, but they could employ different strategies. Once trapped, cancer cells might proliferate within the lumen of the vessel, creating a small tumor that grows and obliterates the adjacent vessel wall. Or, the tumor could push aside endothelial cells and eventually break through the capillary basement membrane, after which the cancer cells invade the parenchyma (Vignjevic and Montagnac, 2008). Alternatively, cancer cells may proceed immediately by squeezing between gaps in the extracellular matrix through amoeboid movements (Sahai, 2005). Finally, the arteries and alveoli of the lung are separated by a relatively thin layer consisting respectively of endothelial cells, a basement membrane and the cuboidal epithelial cells of the alveoli (Guazzi, 2003). Collectively, this may have allowed for podosome-independent invasion. The use of an orthotopic mouse model of cancer in which metastasis is accomplished by cells spreading from the primary tumor, may address which of these models is correct.

A significant percentage of cells in the Tks5 KD tumors expressed high levels of Tks5, implying that the knockdown was not complete at the time of tumor dissection. It is possible that Tks5 expression may have been increasing over time while growing in the mouse (the shRNA vector used does not allow continued selection in vivo). The observation that Tks5 KD subcutaneous tumors eventually increased in volume at a rate similar to the controls could indicate that this is the case. Creating a system in which the investigator can control the levels of Tks5 expression in vivo, in order to maintain knockdown over extended time may overcome this obstacle.

Unexpectedly, and independently of the microenvironment, a reduction in Tks5 was associated with a decreased tumor vascularization. These data may indicate a previously unrealized role for tumor cell podosomes in angiogenesis. It is remains to be established however, whether the differences we observed were related to the reduced size of the Tks5 KD tumors, since a small tumor presumably does not need the same degree of vascularization as a large tumor. On the other hand, restricted angiogenesis could reduce tumor growth. We have also compared the

vessel density and dilation of similarly sized (small) control and Tks5 KD tumors. The vascularization was still reduced in the latter (data not shown), implying that a reduced ability to form podosomes decreases tumor angiogenesis.

In the subcutaneous tumors, reduced vascularization was correlated with a trend to a small increase in apoptosis. It is not clear whether this may have caused the overall decrease in tumor growth, as there was no obvious necrosis in the Tks5 KD tumors (data not shown). On the other hand, a small but long-term increase in apoptosis can cause a sustained decrease in tumor growth. A system in which the investigator is able to reduce Tks5 expression after a tumor has reached a certain size may clarify how podosome formation in cancer cells may determine tumor angiogenesis. One of the major growth factors that regulate tumor angiogenesis is the vascular endothelial growth factor (VEGF) (Duda et al., 2007). Perhaps Tks5, and by implication perhaps podosomes, contribute to the release of VEGF in the microenvironment, thereby promoting angiogenesis to a greater extent in the control tumors compared to the Tks5 KD. However, we did not detect clear differences in VEGF expression between the Tks5 KD and control tumors (data not shown), and we are currently investigating other factors that could explain this phenomenon.

Taken together, our data suggest that a reduction in Tks5 decreases tumor growth in the primary and metastatic site, possibly as a result of decreased podosome/invadopodia formation. Surprisingly, this appeared to be correlated with decreased angiogenesis. These findings support a broader investigation on the impact of Tks5 expression, and podosomes, on tumor progression using different mouse models of cancer.

Acknowledgements

Research support for this work was provided by the National Cancer Institute. Barbara Blouw is supported by fellowship 12FB-0076 of the California Breast Cancer Research Program. We thank Logan Walker, Adriana Charbono and Buddy Charbono for technical assistance, and members of the Courtneidge laboratory for helpful suggestions.

References

Abram CL, Seals DF, Pass I, Salinsky D, Maurer L, Roth TM, Courtneidge SA. The adaptor protein Fish associates with members of the ADAMs family and localizes to podosomes of Src-transformed cells. J. Biol. Chem 2003;278:16844–16851. [PubMed: 12615925]

Artym VV, Zhang Y, Seillier-Moiseiwitsch F, Yamada KM, Mueller SC. Dynamic interactions of cortactin and membrane type 1 matrix metalloproteinase at invadopodia: defining the stages of invadopodia formation and function. Cancer Res 2006;66:3034–3043. [PubMed: 16540652]

Baldassarre M, Pompeo A, Beznoussenko G, Castaldi C, Cortellino S, McNiven MA, Luini A, Buccione R. Dynamin participates in focal extracellular matrix degradation by invasive cells. Mol. Biol. Cell 2003;14:1074–1084. [PubMed: 12631724]

Berdeaux RL, Diaz B, Kim L, Martin GS. Active Rho is localized to podosomes induced by oncogenic Src and is required for their assembly and function. J. Cell Biol 2004;166:317–323. [PubMed: 15289494]

Bharti S, Inoue H, Bharti K, Hirsch DS, Nie Z, Yoon HY, Artym V, Yamada KM, Mueller SC, Barr VA, Randazzo PA. Src-dependent phosphorylation of ASAP1 regulates podosomes. Mol. Cell. Biol 2007;27:8271–8283. [PubMed: 17893324]

Bingle L, Brown NJ, Lewis CE. The role of tumour-associated macrophages in tumour progression: implications for new anticancer therapies. J. Pathol 2002;196:254–265. [PubMed: 11857487]

Blouw B, Song H, Tihan T, Bosze J, Ferrara N, Gerber HP, Johnson RS, Bergers G. The hypoxic response of tumors is dependent on their microenvironment. Cancer Cell 2003;4:133–146. [PubMed: 12957288]

Blouw B, Haase VH, Song H, Bergers G, Johnson RS. Loss of vascular endothelial growth factor expression reduces vascularization, but not growth, of tumors lacking the Von Hippel-Lindau tumor suppressor gene. Oncogene 2007;26:4531–4540. [PubMed: 17297464]

Bowden ET, Barth M, Thomas D, Glazer RI, Mueller SC. An invasion-related complex of cortactin, paxillin and PKCmu associates with invadopodia at sites of extracellular matrix degradation. Oncogene 1999;18:4440–4449. [PubMed: 10442635]

Bowden ET, Onikoyi E, Slack R, Myoui A, Yoneda T, Yamada KM, Mueller SC. Co-localization of cortactin and phosphotyrosine identifies active invadopodia in human breast cancer cells. Exp. Cell Res 2006;312:1240–1253. [PubMed: 16442522]

Chellaiah MA. Regulation of podosomes by integrin alphavbeta3 and Rho GTPase-facilitated phosphoinositide signaling. Eur. J. Cell Biol 2006;85:311–317. [PubMed: 16460838]

Clark ES, Whigham AS, Yarbrough WG, Weaver AM. Cortactin is an essential regulator of matrix metalloproteinase secretion and extracellular matrix degradation in invadopodia. Cancer Res 2007;67:4227–4235. [PubMed: 17483334]

Duda DG, Batchelor TT, Willett CG, Jain RK. VEGF-targeted cancer therapy strategies: current progress, hurdles and future prospects. Trends Mol. Med 2007;13:223–230. [PubMed: 17462954]

Gimona M, Buccione R. Adhesions that mediate invasion. Int. J. Biochem. Cell Biol 2006;38:1875–1892. [PubMed: 16790362]

Gimona M, Buccione R, Courtneidge SA, Linder S. Assembly and biological role of podosomes and invadopodia. Curr. Opin. Cell Biol. 2008in press.

Guazzi M. Alveolar-capillary membrane dysfunction in heart failure: evidence of a pathophysiologic role. Chest 2003;124:1090–1102. [PubMed: 12970042]

Linder S, Aepfelbacher M. Podosomes: adhesion hot-spots of invasive cells. Trends Cell Biol 2003;13:376–385. [PubMed: 12837608]

Lock P, Abram CL, Gibson T, Courtneidge SA. A new method for isolating tyrosine kinase substrates used to identify fish, an SH3 and PX domain-containing protein, and Src substrate. EMBO J 1998;17:4346–4357. [PubMed: 9687503]

Orimo A, Weinberg RA. Stromal fibroblasts in cancer: a novel tumor-promoting cell type. Cell Cycle 2006;5:1597–1601. [PubMed: 16880743]

Sahai E. Mechanisms of cancer cell invasion. Curr. Opin. Genet. Dev 2005;15:87–96. [PubMed: 15661538]

Seals DF, Azucena EF Jr, Pass I, Tesfay L, Gordon R, Woodrow M, Resau JH, Courtneidge SA. The adaptor protein Tks5/Fish is required for podosome formation and function, and for the protease-driven invasion of cancer cells. Cancer Cell 2005;7:155–165. [PubMed: 15710328]

Steeg PS. Tumor metastasis: mechanistic insights and clinical challenges. Nat. Med 2006;12:895–904. [PubMed: 16892035]

Vignjevic D, Montagnac G. Reorganisation of the dendritic actin network during cancer cell migration and invasion. Semin. Cancer Biol 2008;18:12–22. [PubMed: 17928234]

Vishnubhotla R, Sun S, Huq J, Bulic M, Ramesh A, Guzman G, Cho M, Glover SC. ROCK-II mediates colon cancer invasion via regulation of MMP-2 and MMP-13 at the site of invadopodia as revealed by multiphoton imaging. Lab. Invest 2007;87:1149–1158. [PubMed: 17876296]

Weaver AM. Invadopodia: specialized cell structures for cancer invasion. Clin. Exp. Metastasis 2006;23:97–105. [PubMed: 16830222]

Yamaguchi H, Lorenz M, Kempiak S, Sarmiento C, Coniglio S, Symons M, Segall J, Eddy R, Miki H, Takenawa T, Condeelis J. Molecular mechanisms of invadopodium formation: the role of the N-WASP-Arp2/3 complex pathway and cofilin. J. Cell Biol 2005;168:441–452. [PubMed: 15684033]

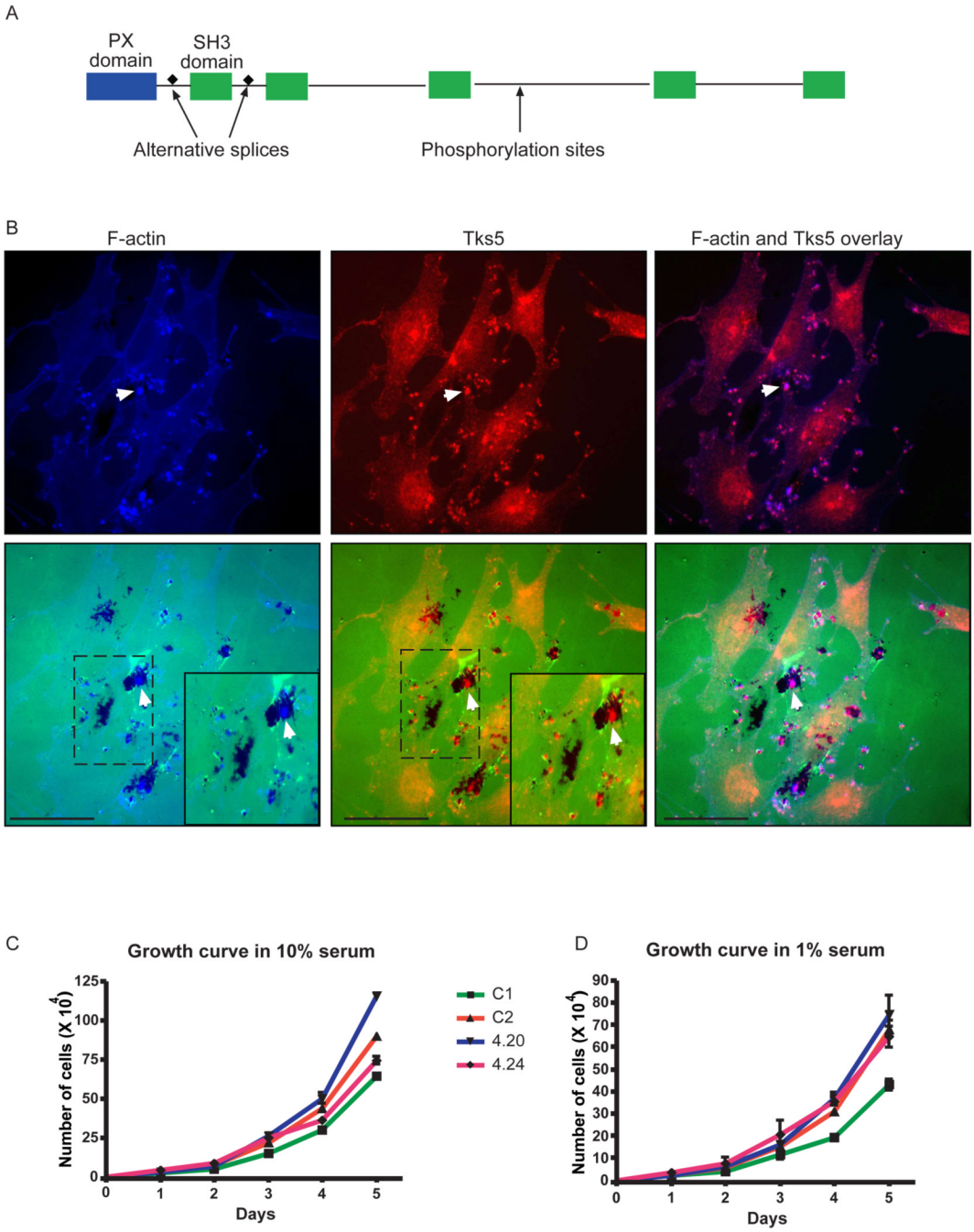

Fig. 1. The scaffold protein Tks5 co-localizes to podosomes in Src-transformed fibroblasts and mediates gelatin degradation

(A) The primary structure of Tks5, showing an amino-terminal phox homology (PX) domain (blue box) and five SH3 domains (green boxes). Tks5 is tyrosine phosphorylated in Src-transformed fibroblasts (the phosphorylation sites are indicated by an arrow) and has two alternative splicing sites (squares). (B) Top panels: F-actin morphology of Src-transformed fibroblasts (in blue, left panel) shows podosomes (indicated by white arrow). Tks5 co-localizes to these structures as shown by a white arrow in the middle and right panel (overlay of F-actin and Tks5). Lower panels: overlay of FITC gelatin with respectively F-actin, Tks5 and both F-actin and Tks5. Bars: 100 μm. Insets: magnification of the regions within the dashed boxes,

showing in detail respectively gelatin degradation at sites of podosomes (left panel) and co-localization of Tks5 to these specific areas (middle and right panel). (C, D) Growth curves of Src-transformed fibroblasts under respectively 10% and 1% serum conditions.

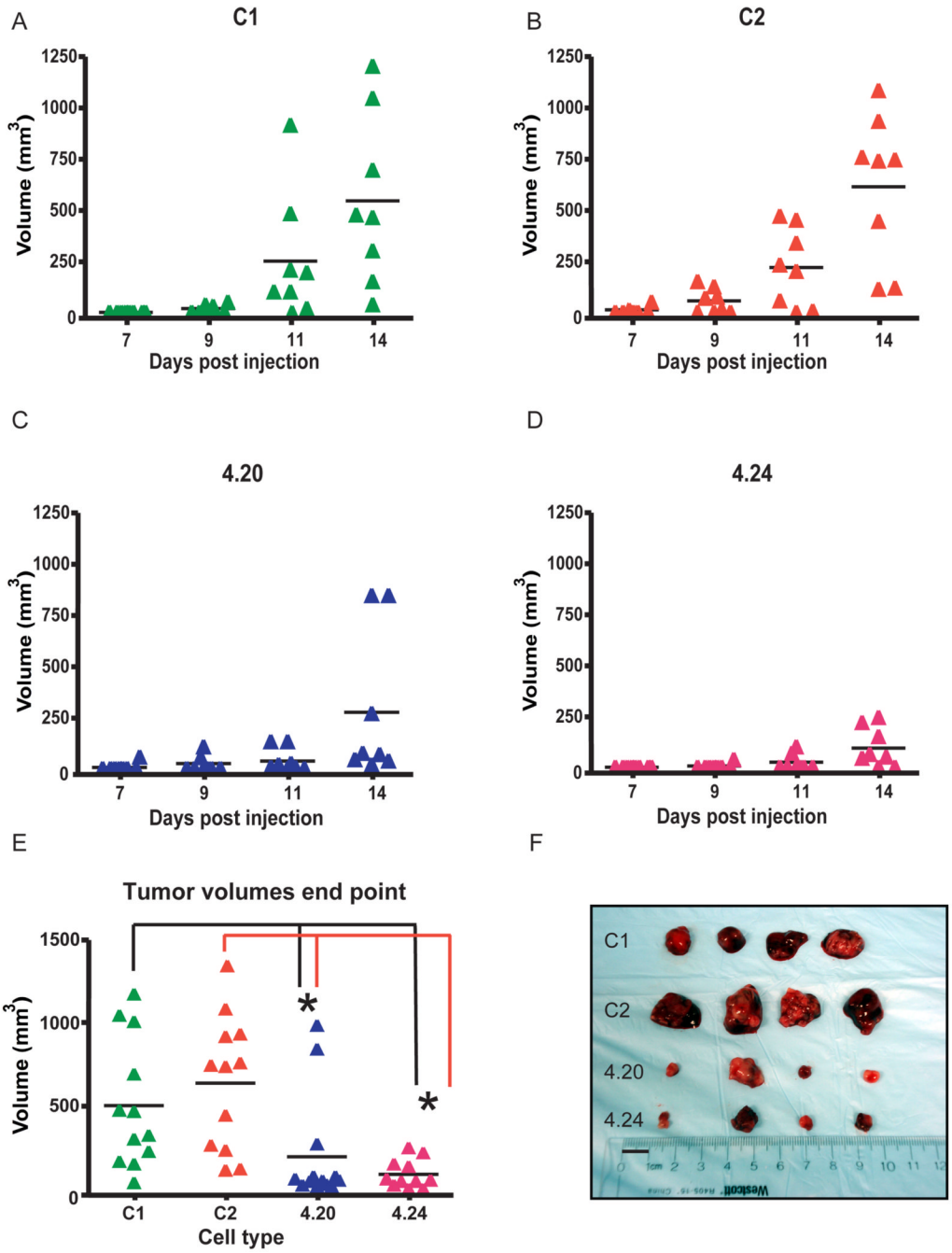

Fig. 2. Decreased expression of Tks5 impairs subcutaneous tumor growth

(A – D) Two Tks5 KD clones 4.20 and 4.24 and two controls, C1 and C2 were grown over a 14-day time period, and every 2–3 days volumes were determined as described in Materials and methods. N = 8 mice per tumor type. (E) Tumor volumes at the end point of the assay (day 14 post injection). Values were calculated of 3 independent experiments, * $p < 0.05$ and n = 12. Scatter plots indicate Mean ± SEM. (F) Photographs of 4 tumors per group at the day of dissection. The image is representative of all experiments performed. Bar: 1 cm.

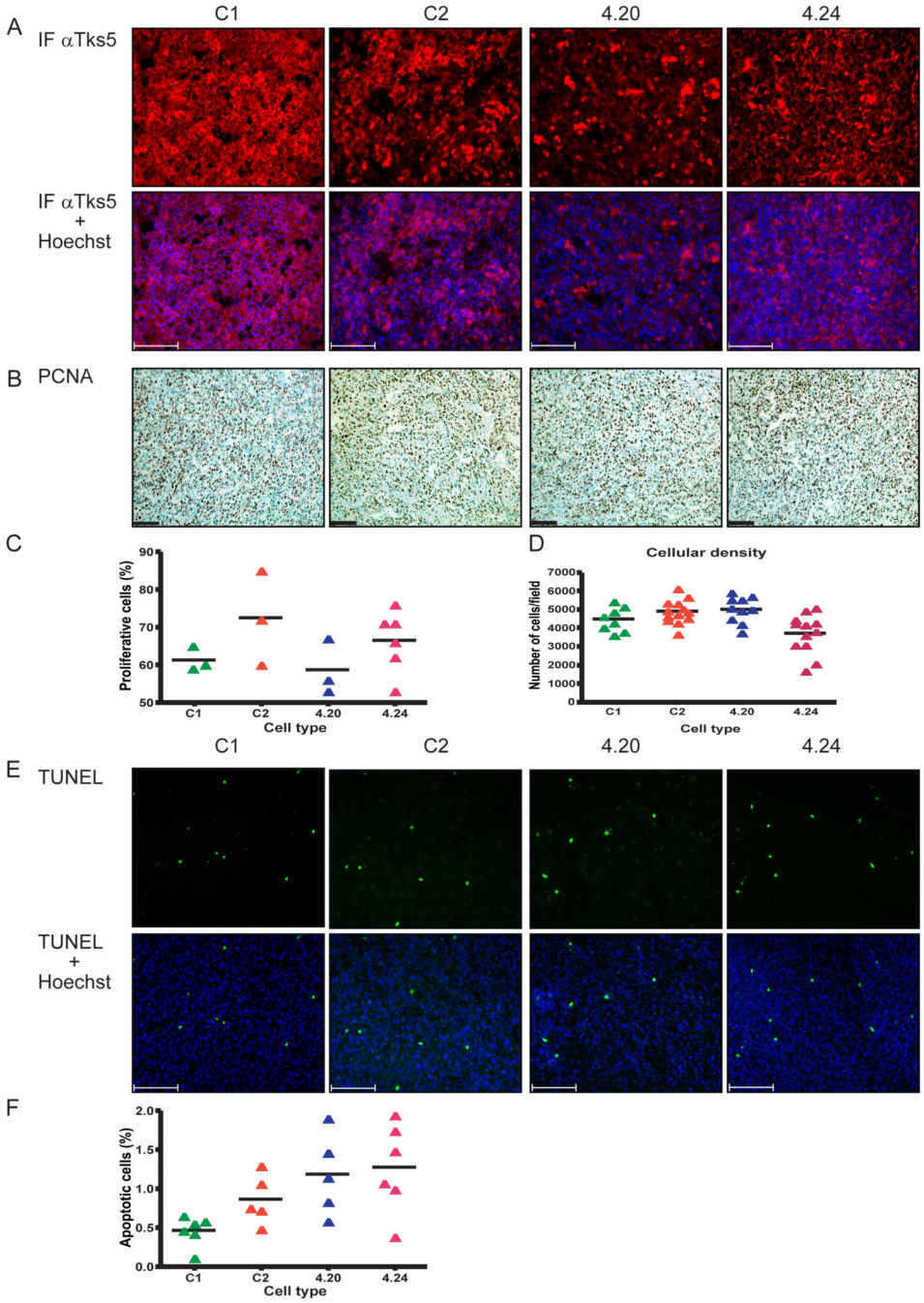

Fig. 3. Tumor proliferation and apoptosis is not significantly altered by Tks5 knockdown

(A) Top panels: Tks5 expression was visualized by immunofluorescence (intense red). Note the decreased fraction of 4.20 cells with similar intensity of Tks5 expression as the controls, indicating an overall decreased expression of Tks5 in these tumors. Lower panel: overlay of Tks5 and Hoechst. (B) Images of PCNA immunohistochemistry performed on sections of the subcutaneous tumors. PCNA was developed in DAB (brown) followed by a counterstain with methylgreen (blue-green). (C) Scatterplot showing the proliferation rate that was determined based on the PCNA staining. (D) Scatterplot showing the cellular density of the SC tumors as determined by the number of nuclei per 10× field, of at least 2–3 different tumors per group and 6 to 7 fields per tumor. (E) Top panels: images of cell death in the SC tumors indicated by

TUNEL staining. Lower panels: overlay of TUNEL with Hoechst. (F) Scatterplot of the apoptotic rate that was calculated based on the TUNEL images. Quantification of the proliferation and apoptotic rate was carried out using ImagePro software as described in Materials and methods. Scatterplots indicate mean ± SEM. Bars: 100 μm, for all images and the photographs are representative of all tumors per group.

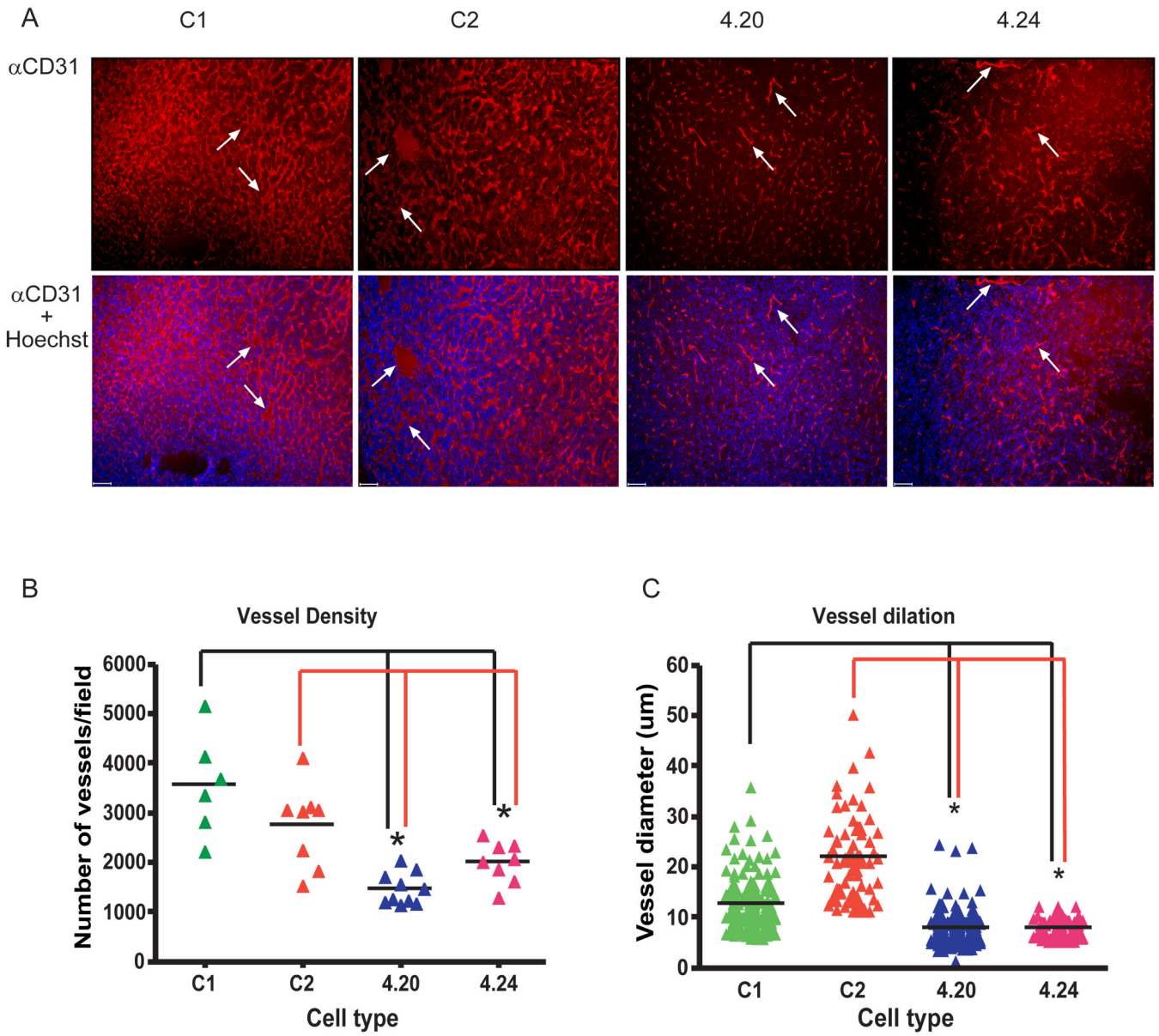

Fig. 4. Tks5 KD tumors show a reduced vascularization compared to controls

(A) Vessel morphology and density was visualized by a staining for CD31 on frozen sections obtained from the tumors. The Tks5 KD tumors displayed reduced vessel dilation (compare vessel width of those indicated by the white arrows in the 4.20 and 4.24 with those in the C1 and C2 tumors, top panels) and a less complex vessel network. Lower panels show overlay of CD31 with Hoechst. Bars: 100 μm. (B) Scatterplot of the vessel density that was calculated based on the CD31 immunofluorescence images. (C) Scatterplot of the vessel diameter. Quantification of the vessel density and dilation was carried out as described in Materials and methods, using ImagePro software, and the plots display the mean ± SEM,* is $p < 0.05$ and $n = 6–10$ (n being the number of tumors per group).

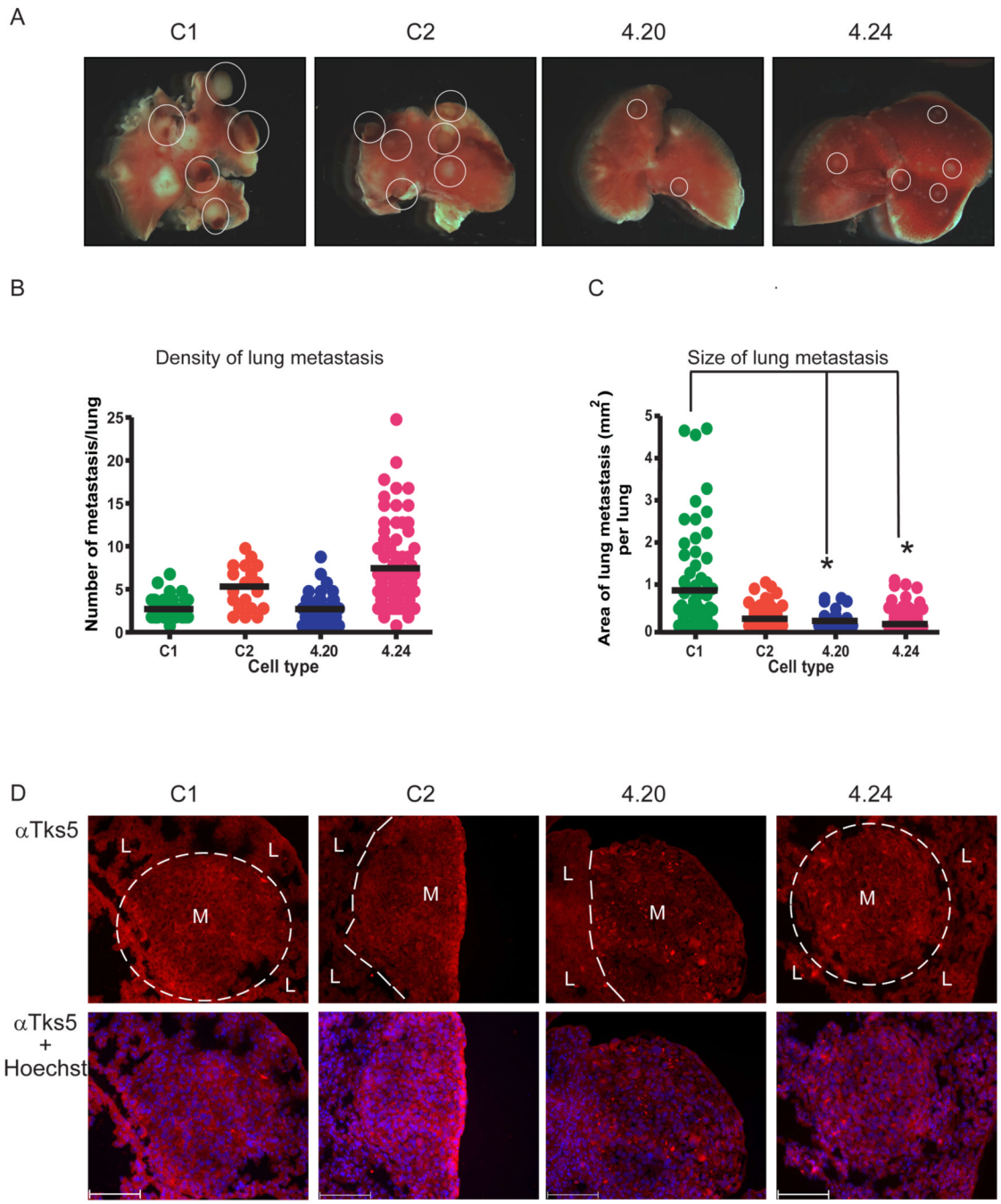

Fig. 5. Reduction in Tks5 decreases the size of metastatic lesions

(A) Images of the right lung lobe of each tumor group. Metastatic lesions are indicated as yellow-white nodules (some of which are circled) whereas the normal lung parenchyma is pink. Each photograph is representative of the entire tumor group. (B) Scatterplot showing the number of metastases per lung. (C) Scatterplot showing the size of metastasis per lung (4 lungs per groups were analyzed). Values for the metastatic density and size were obtained and calculated as described in Materials and methods. The plots indicate the mean ± SEM. * $p < 0.05$. (D) Top panels: Tks5 detection on frozen sections. Metastases (M) are distinguished by dashed lines from the normal lung parenchyma (L). Lower panels: Tks5 immunofluorescence overlay with Hoechst. Bars: 100 μm,

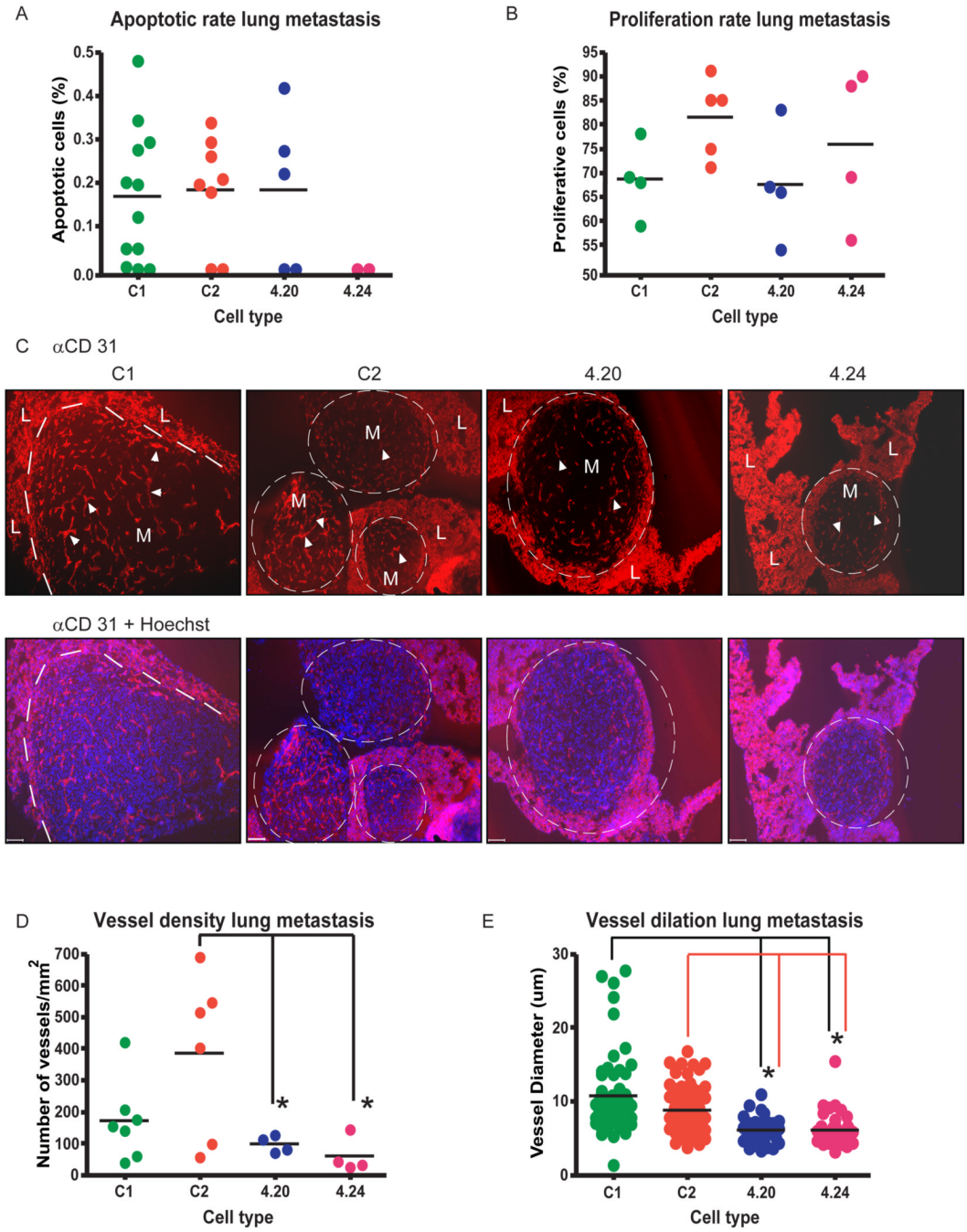

Fig. 6. Angiogenesis, but not viability, is reduced in the Tks5 KD lung metastases

(A) Scatterplot showing the apoptotic rate which was calculated based on the TUNEL staining of lung sections. Note that only 2 metastatic lesions were present in the lungs of the mouse injected with the 4.24 cells. (B) Scatterplot showing the proliferation rate that was calculated based on PCNA staining on lung sections. (C) Vessel morphology and density was visualized by CD31 immunofluorescence. The Tks5 lung metastatic lesions showed reduced vessel dilation, compare vessels indicated by the white arrowheads in the metastatic lesions (M) of the 4.20 and 4.24 metastases to the controls. Top panels: CD31 immunofluorescence, lower panels; overlay with Hoechst. Bars: 100 μm. (D) Scatterplot showing the vessel density indicating a trend towards a reduced vessel density in the Tks5 KD metastases. $p < 0.05$ for

4.20 and 4.24 compared to C2, n = 8 tumors per group. (E) Scatter plot of the vessel diameter indicating a decrease in vessel dilation in the Tks5 KD lung lesions. $p < 0.05$. At least 30 vessels per metastasis were analyzed, using 4 tumor types per group.